Protein Science (1996), 5:1816–1825. Cambridge University Press. Printed in the USA.

An optimized **g**-tensor for *Rhodobacter capsulatus* cytochrome c_2 in solution: A structural comparison of the reduced and oxidized states

DEZHENG ZHAO,[1] HAROLD M. HUTTON,[2] MICHAEL A. CUSANOVICH,[3] AND NEIL E. MACKENZIE[1]

[1] Department of Pharmacology & Toxicology, College of Pharmacy, University of Arizona, Tucson, Arizona 85721
[2] Chemistry Department, University of Winnipeg, Winnipeg, Manitoba R3B 2E9, Canada
[3] Department of Biochemistry, University of Arizona, Tucson, Arizona 85721

(RECEIVED April 10, 1996; ACCEPTED May 24, 1996)

Abstract

The optimized **g**-tensor parameters for the oxidized form of *Rhodobacter capsulatus* cytochrome c_2 in solution were obtained using a set (50) of backbone amide protons. Dipolar shifts for more than 500 individual protons of *R. capsulatus* cytochrome c_2 have been calculated by using the optimized **g**-tensor and the X-ray crystallographic coordinates of the reduced form of *R. capsulatus* cytochrome c_2. The calculated results for dipolar shifts are compared with the observed paramagnetic shifts. The calculated and the observed data are in good agreement throughout the entire protein, but there are significant differences between calculated and experimental results localized to the regions in the immediate vicinity of the heme ligand and the region of the front crevice of the protein (residues 44–50, 53–57, and 61–68). The results not only indicate that the overall solution structures are very similar in both the reduced and oxidized states, but that these structures in solution are similar to the crystal structure. However, there are small structural changes near the heme and the rearrangement of certain residues that result in changes in their hydrogen bonding concomitant with the change in the oxidation states; this was also evident in the data for the NH exchange rate measurements for *R. capsulatus* cytochrome c_2.

Keywords: cytochrome c_2; **g**-tensor; NMR; paramagnetic shift

Rhodobacter capsulatus cytochrome c_2, a member of the class I *c*-type cytochromes, acts as an electron carrier for both the photosynthetic and respiratory pathways. There have been many studies of *R. capsulatus* cytochrome c_2 in an attempt to understand the structure–function relationship, including global stability (Cusanovich et al., 1988), mutant studies (Caffrey et al., 1992), X-ray structure (Benning et al., 1991), and the hydrogen exchange behavior by NMR spectroscopy (Gooley et al., 1991). These results have been compared with those of other cytochromes *c*, such as tuna (Takano & Dickerson 1981a, 1981b), horse (Englander & Kallenbach, 1984), yeast (Cutler et al., 1987), and *Rhodospirillium rubrum* (Salemme et al., 1973; Bhatia, 1981). Recently an alternative approach to the redox-dependent structural changes for horse cytochrome *c* has been examined (Feng et al., 1990) using an optimized **g**-tensor determined from a set of $C_\alpha H$ proton chemical shifts of the reduced and oxidized forms of the cytochrome and the coordinates of the protons relative to the heme iron in the crystallographic structure. The calculated **g**-tensor was used to determine the pseudocontact shifts of the assigned protons of ferricytochrome *c* and hence any redox dependent structural change(s) could be assessed. Further, the paramagnetic effects on the NMR chemical shifts could be introduced as constraints in energy minimization or molecular dynamic calculations in the NMR solution structure refinement (Gochin & Roder, 1995).

Iron exists in two physiologically important oxidation states in cytochrome c_2; the reduced form is diamagnetic [Fe(II), low spin d^6, $S = 0$] and the oxidized form is paramagnetic [Fe(III), low spin d^5, $S = 1/2$]. As a consequence of the unpaired electron in ferricytochrome c_2, the hyperfine chemical shifts, which includes the Fermi contact and the pseudocontact shifts, will affect the proton chemical shifts in the oxidized state. The observed chemical shift differences for individual protons in the two redox states are dependant on these contact shifts and any diamagnetic shifts due to structural changes. They can be represented as follows (Feng et al., 1990):

$$\Delta obs = \delta_{ox} - \delta_{red} = \Delta c + \Delta pc,x + \Delta s \quad (1A)$$

$$\Delta obs = \delta_{ox} - \delta_{red} = \Delta pc,x + \Delta s, \quad (1B)$$

Reprint requests to: Neil E. MacKenzie, Department of Pharmacology & Toxicology, College of Pharmacy, University of Arizona, Tucson, Arizona 85721; e-mail: dzhao@ccit.arizona.edu.

where δ_{ox} and δ_{red} are the measured chemical shifts in the two different oxidation states, Δc is the Fermi contact contribution to the chemical shift, $\Delta pc,x$ represents the pseudocontact contribution, and Δs is the diamagnetic chemical shift due to any redox dependent structural change. Due to the rapid attenuation with an increase in the number of intervening bonds, the Fermi contact shift is limited to protons on the heme and the covalently bonded residues; Equation 1B would apply to all groups of substituents that are *not* attached to the heme.

For the protons in the ferricytochrome c_2, the pseudocontact shifts are determined by (Kurland & McGarvey, 1970; Horrocks & Greenberg, 1973):

$$\Delta pc,x = [\beta^2 S(S+1)/9kTr^3] \times [g_{ax}(3\cos^2\theta - 1) + 1.5\, g_{eq}(\sin^2\theta \cos 2\phi)], \quad (2A)$$

$$g_{ax} = g_z^2 - 1/2(g_x^2 + g_y^2), \quad (2B)$$

$$g_{eq} = g_x^2 - g_y^2, \quad (2C)$$

where β is the Bohr magneton, S is the electron spin quantum number, k represents the Boltzmann constant, T is the absolute temperature, (r, θ, ϕ) represent the coordinates of the position of each proton, (g_x, g_y, g_z) are the electronic **g**-tensor parameters, and (g_{ax}, g_{eq}) are the axial and equatorial anisotropies of the **g**-tensor. The **g**-tensor principal axis system is defined by the three Euler angles, α, β, γ, with respect to the heme coordinates as described previously (Feng et al., 1990) and shown in Figure 1.

In general, from the parameters of the optimized **g**-tensor for *R. capsulatus* cytochrome c_2 in solution, the dipolar shifts $(\Delta pc,x)$ can be calculated for each proton in the molecule. A comparison of these calculated dipolar shifts, $\Delta pc,x$, with the observed paramagnetic shifts that occur with a change in the oxidation state, $\Delta obs = \delta_{ox} - \delta_{red}$, would indicate which residues in this molecule have or have not undergone significant structural changes with a change of oxidation state.

The backbone ^{1}H and ^{15}N NMR assignments of both the reduced and oxidized forms have been completed (Gooley et al., 1990; D. Zhao, P.R. Gooley, M.A. Cusanovich, N.E. MacKenzie, unpubl.). In this paper, we present the determination of an optimized **g**-tensor for the *R. capsulatus* cytochrome c_2 in solution, and the calculation of the dipolar shifts $(\Delta pc,x)$ for the protons of cytochrome c_2 using the optimized **g**-tensor and the X-ray crystallographic coordinates of reduced *R. capsulatus* cytochrome c_2 (Benning et al., 1991). The difference between the calculated and observed paramagnetic shifts for the cytochrome c_2 can be indicative of structural changes of the protein between the two oxidation states in solution and/or between the crystal and the solution.

Results

The optimized **g**-tensor components g_{ax}, g_{eq}, α, β, and γ for *R. capsulatus* cytochrome c_2 were obtained using the least-squares fitting method on 50 reference NH protons by minimizing the variance χ^2/N (N is the number of residues) to the value 0.001. The heme-related groups and the optimized **g**-tensor system are shown in Figure 1, using the original set of 50 NH protons chosen by the amide group chemical shift synchronization (see Materials and methods). The initial and final optimized **g**-tensor parameters are given in Table 1. The values of the anisotropy, g_{ax} and g_{eq}, differ slightly from those determined by others for various species of cytochromes (Mailer & Taylor, 1972; Williams et al., 1985; Feng et al., 1990; Gao et al., 1991; Timkovich & Cai, 1993). For the orientation of the **g**-tensor, β was offset by 12 degrees from the original z axis, orienting the g_z approximately along the Met-96 S_δ-Fe bond. The sum of α and γ is equal to approximately 360 degrees, indicating that g_x and g_y remain aligned along the x,y axes (Fig. 1) in the plane of the heme system.

The calculated dipolar shifts for backbone NH and $C_\alpha H$ protons, respectively, as a function of the residue number are shown in Figure 2. The calculated dipolar shifts cover a range of approximately 9 ppm, from 6 to −3 ppm, and are accurate to ±0.02 ppm. Regions of the protein that are in the vicinity of the heme can exhibit large positive or negative dipolar shifts values. The pseudocontact shift values for folded cytochromes change from positive to negative, or vice versa, four times, as can be seen from the plot in Figure 2. However, there is an exception for the positive region from 93–99, as there are negative values: −1.28, for Ala-97 in the NH plot and −0.81 and −2.13, for Gly-95 and Met-96, respec-

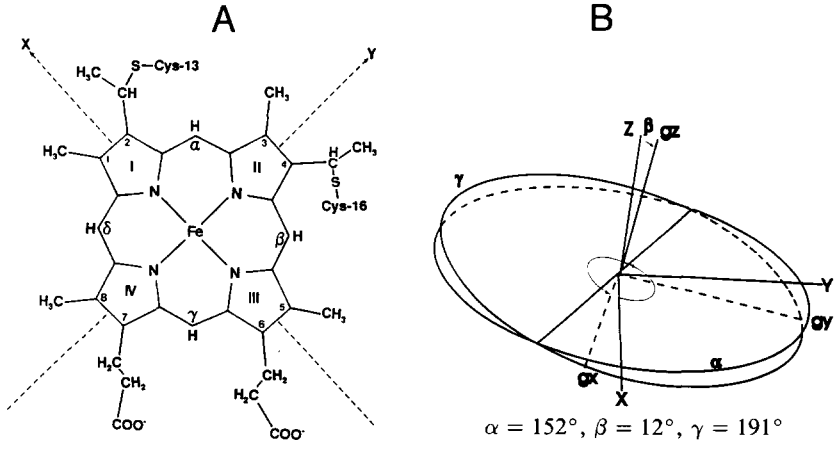

Fig. 1. Heme-related groups (**A**) and optimized **g**-tensor system (**B**). x and y axes of the heme-based coordinate system, viewed from Met-96, are indicated; z axis is normal to the heme plane. The orientation of the optimized **g**-tensor principal axial system (g_x, g_y, and g_z) relative to the heme coordinate system is defined by three Eular angles, α, β, and γ.

Table 1. *g-Tensor parameters*

Source	Principal axes $g_x\ g_y\ g_z$	Anisotropy $g_{ax}\ g_{eq}$	Orientation $\alpha\ \beta\ \gamma$	χ^2/N[a]
EPR[b]	1.25, 2.25, 3.06	6.05, −3.50	0°, 0°, 0°	
Tuna[c]		5.24, −2.91	$\alpha+\gamma = 358°$, $\beta = 11°$	
Horse (64C_αH)[d]	2.25, 2.59, 3.32	5.15, −1.65	106°, 13°, 251°	0.004
Yeast[e]		4.58, −2.31	$\alpha+\gamma = 366°$, $\beta = 9°$	
R. capsulatus				
(50NH)	2.24, 2.47, 3.26	4.80, −1.0	152°, 12°, 191°	0.001
(45NH)		4.80, −1.0	153°, 12°, 190°	0.001
(43NH)		4.70, −1.0	154°, 12°, 192°	0.001

[a] The statistical variance, with χ^2 defined as in Equation 6.
[b] Mailer and Taylor (1972).
[c] Williams et al. (1985).
[d] Feng et al. (1990).
[e] Gao et al. (1991).

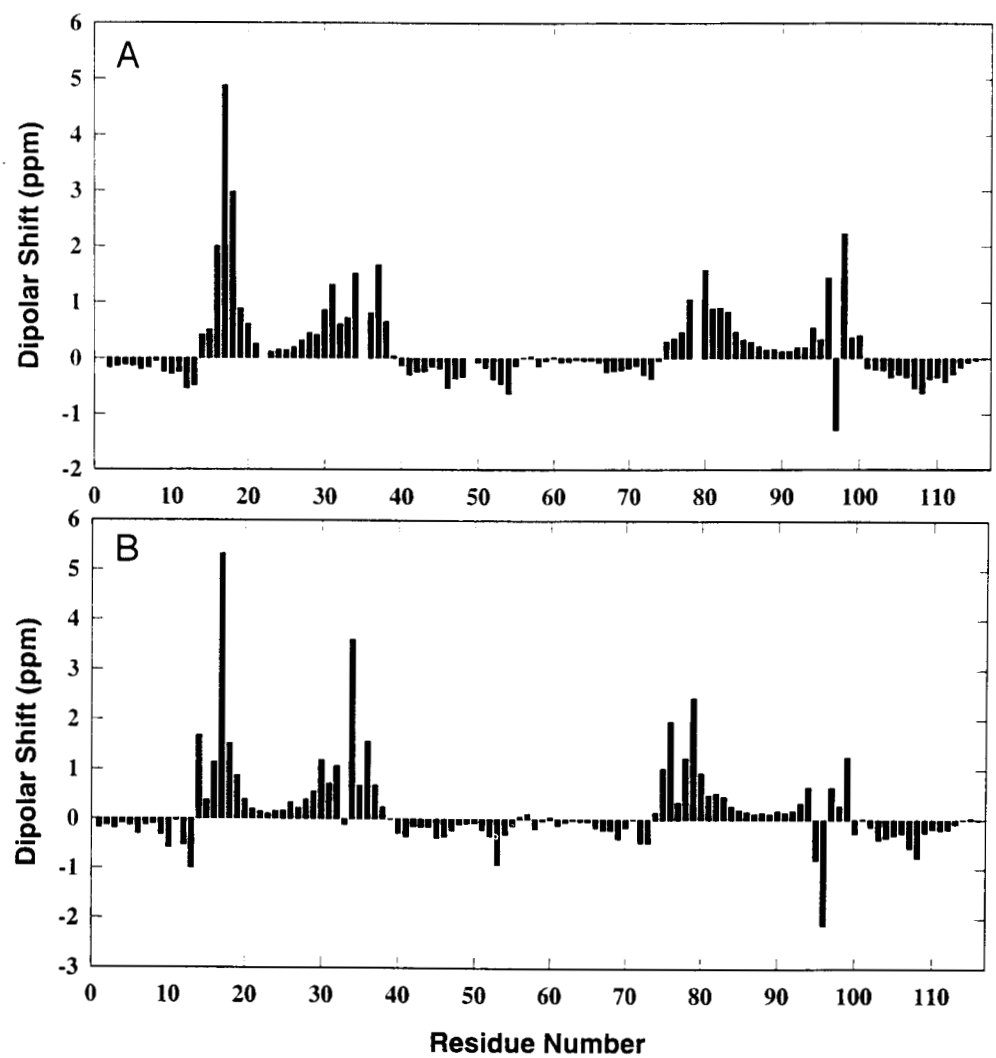

Fig. 2. Calculated dipolar shifts as a function of residue number for backbone amide protons (**A**) and α protons (**B**), respectively. In the latter, only the α_1H protons of glycines, according to the Brookhaven Protein Data Bank, were shown here.

tively, in the αH plot. These values are consistent with the experimental chemical shift values that are given as a function of residue number in Figure 3.

The dipolar chemical shifts for more than 500 protons (of the ~600 assigned protons), including backbone NH, $C_\alpha H$, $C_\beta H$, and other protons, were calculated for *R. capsulatus* cytochrome c_2 using the optimized **g**-tensor and compared with their observed paramagnetic shifts. For the $C_\alpha H_2$ of glycines and $C_\beta H_2$ of meth-

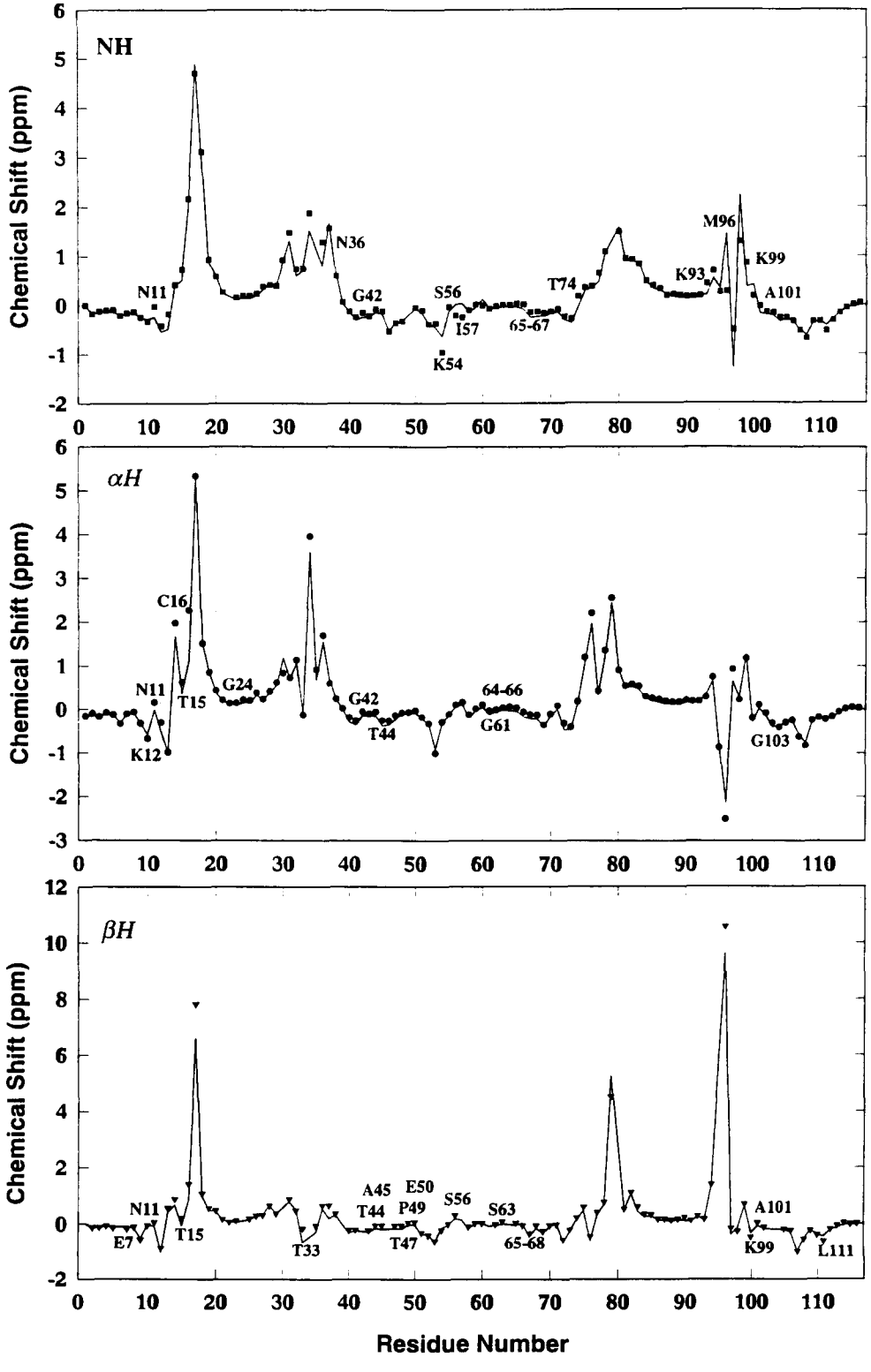

Fig. 3. Calculated dipolar shifts (curves) and observed paramagnetic shifts for backbone amide protons (■), α protons (●), and β protons (▼) as a function of the residue numbers, respectively. Labeled residues are those protons selected by Equation 8 from Table 2.

ylene groups and for the paired methyl groups of valines and leucines, the stereospecific resonance assignments could often be made by matching the observed experimental values with the calculated dipolar values for the two ambiguous protons. For methyl groups and fast-flipping aromatic rings and some $C_\gamma H_2$, $C_\delta H_2$, $C_\epsilon H_2$ methylene groups that are in fast stereochemical exchange with respect to the NMR time scale, the average position in the X-ray coordinate was used for the calculated pseudocontact shifts. A comparison of the calculated dipolar chemical shifts with observed paramagnetic shifts for backbone NH, $C_\alpha H$, and $C_\beta H$ protons as a function of residue number are shown in Figure 3. Plot of observed experimental versus calculated pseudocontact shifts for NH (Fig. 4A) and for $C_\alpha H$ (Fig. 4B) of *R. capsulatus* cytochrome c_2 are shown in Figure 4. A qualitative estimation of the fit between the calculated and observed values with respect to residue number can be made from Figures 3 and 4. Regions in which the calculated and observed results agreed very well are known to be the most rigid parts of the molecule, 2–10 (N-terminal helix), 19–29 (Ω loop), 83–92 (helix), 102–115 (C-terminal helix), whereas the residues located in the vicinity of the heme group are markedly different.

Protons that appear to experience significant structural change are listed in Table 2; these protons are found in regions that span residues 44–50, 53–57, and 61–68, as well as others in the immediate vicinity of the heme ligand. The results will be discussed below.

Discussion

In this study, an optimized **g**-tensor was obtained from a set of 50 NH protons selected using the criterion of the amide group chemical shift synchronization. In conjunction with the X-ray crystal coordinates of the reduced *R. capsulatus* cytochrome c_2, the dipolar shifts were calculated for the majority (~90%) of the assigned protons in the protein. For extensive portions of the protein, there is excellent agreement between calculated and observed shifts, indicating that there is structural fidelity between crystal and solution structures and between the two oxidation states. This agrees with the qualitative analysis of proton NOE data and NH exchange rate data for *R. capsulatus* cytochrome c_2 (Gooley et al., 1991; D. Zhao, P.R. Gooley, M.A. Cusanovich, M.E. MacKenzie, unpubl.), and with the crystallographic data (Takano & Dickerson, 1981a, 1981b) and other NMR studies (Williams et al., 1985; Feng et al., 1989; Wand et al., 1989; Gao et al., 1991).

However, several regions in the folded protein that are connected with the heme group were found to be affected significantly by the change in oxidation state. In Table 2, the differences between the calculated and experimental chemical shift values are given for those protons in the sequences that are indicated by Equation 8 to have a significant structural change. An α-carbon model of *R. capsulatus* cytochrome c_2 from the crystal coordinates of ferrocytochrome c_2 (Benning et al., 1991) is presented in Figure 5 in order to assist in the understanding of the distribution of the residues listed in Table 2. Those residues showing significant deviations from the calculated chemical shift will be grouped into three regions for discussion.

Using the α-carbon model given in Figure 5, the region on the right side of the heme, which includes the six residues Asn-11, Lys-12, Thr-15, Cys-16, Thr-33, and Asn-36 are in close proximity to one of the two axial ligands of the heme iron, Fe-N (imino nitrogen of His-17), and its immediate environment. In the folded protein, several hydrogen bonds in this region are important, such as Gly-34(NH) to Cys-16(CO), Ala-31(NH) to Lys-14(CO), and the imidazole group $N_\pi H$ of His-17 to Pro-35(CO), as well as axial ligand and the bonds between heme and Cys-13 and Cys-16. The local structural or conformational changes in this region may reflect the changes that occur in the heme porphyrin group and/or the

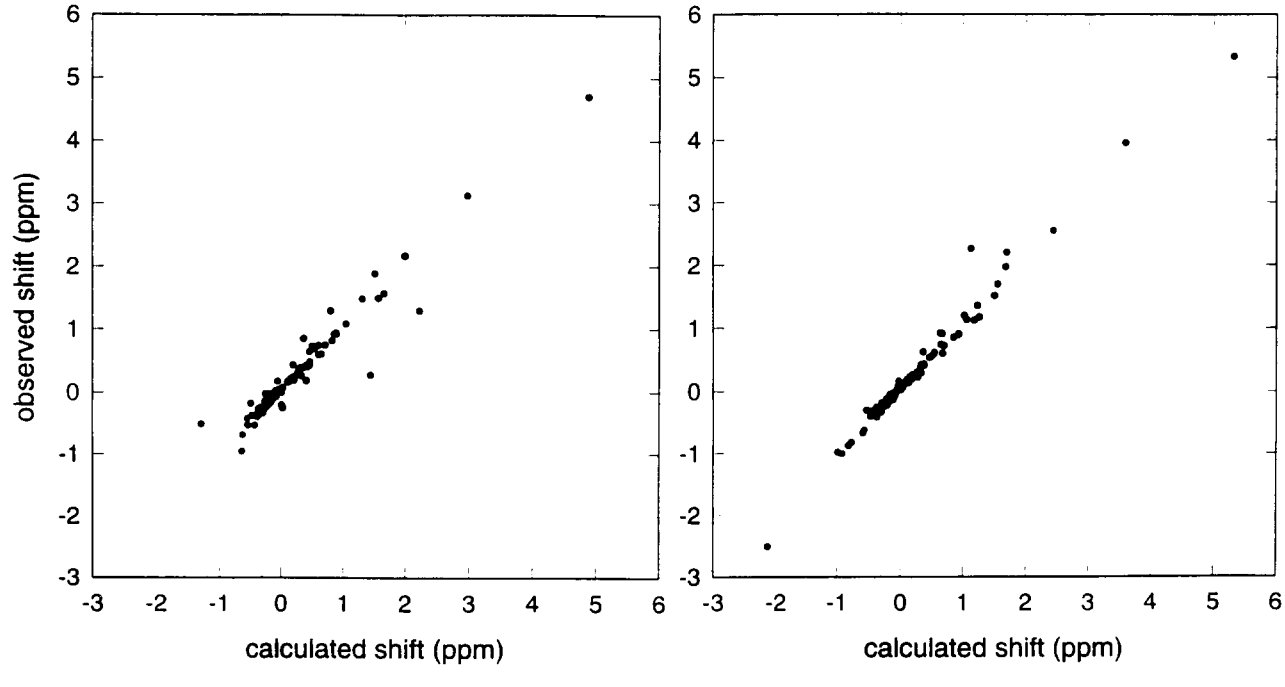

Fig. 4. Plots of observed experimental versus calculated pseudocontact shifts (**A**) for backbone amide protons and (**B**) for α protons of *R. capsulatus* cytochrome c_2.

Table 2. *Protons that show significant differences between calculated dipolar shift and observed paramagnetic shift*[a]

Proton		Obs (ppm)[b] ox–red	Calc (ppm)[c] $\Delta pc,x$	Diff (ppm) obs − calc	$\delta\Delta pc$ (ppm)[d] (δl = 0.3 Å)
Glu-7	βH	−0.18	−0.09	−0.09	0.02
Asn-11	NH	−0.03	−0.25	0.22	0.05
	αH	0.15	−0.02	0.17	0.04
	β_1H	0.06	−0.08	0.14	0.03
	δ_1H	−0.03	−0.34	0.31	0.05
	δ_2H	0.03	−0.27	0.30	0.03
Lys-12	αH	−0.31	−0.53	0.22	0.10
	β_2H	−0.71	−0.99	0.28	0.14
Thr-15	αH	0.62	0.37	0.25	0.09
	β_1H	0.22	−0.07	0.29	0.15
	γH_3[e]	0.08	−0.16	0.24	0.07
Cys-16	αH	2.26	1.13	1.13	0.37
Gly-24	α_1H	0.22	0.15	0.07	<0.01
Thr-33	βH	−0.16	−0.65	0.49	0.16
	γH_3[e]	−0.74	−0.11	−0.63	0.06
Asn-36	NH	1.29	0.80	0.49	0.17
Gly-42	NH	−0.15	−0.25	0.10	0.02
	α_1H	−0.06	−0.14	0.08	0.01
Thr-44	αH	−0.06	−0.16	0.10	0.01
	βH	−0.05	−0.14	0.09	<0.01
Ala-45	βH_3[e]	−0.05	−0.19	0.14	0.04
Thr-47	βH	−0.05	−0.15	0.10	0.01
	γH_3[e]	−0.08	−0.17	0.09	0.01
Tyr-48	δH_2[e]	0.23	0.04	0.19	0.04
Pro-49	β_1H	0.06	−0.03	0.09	<0.01
Glu-50	β_1H	0.08	−0.02	0.10	0.01
Tyr-53	δ_1H	−0.29	−0.45	0.16	0.05
	δ_2H	−0.93	−1.17	0.24	0.20
	ϵ_2H	−0.47	−1.42	0.95	0.27
Lys-54	NH	−0.96	−0.64	−0.32	0.11
Ser-56	NH	−0.21	0.01	−0.22	0.02
	β_1H	0.32	0.20	0.12	0.03
Ile-57	NH	−0.25	0.04	−0.29	0.05
	βH	0.79	0.15	0.64	0.11
Gly-61	α_1H	0.03	−0.09	0.12	0.01
	α_2H	0.03	−0.08	0.11	0.01
Ser-63	β_1H	0.10	0.01	0.09	<0.01
	β_2H	0.11	0.01	0.10	<0.01
Gly-64	α_1H	0.06	−0.04	0.10	<0.01
	α_2H	0.03	−0.05	0.08	<0.01
Phe-65	NH	0.04	−0.04	0.08	<0.01
	αH	0.03	−0.05	0.08	<0.01
	β_1H	0.05	−0.03	0.08	0.01
	β_2H	0.07	−0.01	0.08	<0.01
	δH_2[e]	0.10	−0.02	0.12	0.01
	ϵH_2[e]	0.12	−0.01	0.13	0.02
	ζH	0.11	−0.01	0.11	0.03
Ala-66	NH	0.02	−0.09	0.11	0.01
	αH	−0.07	−0.17	0.10	0.02
	βH_3[e]	−0.05	0.02	−0.07	<0.01
Trp-67	NH	−0.14	−0.25	0.11	0.03
	δ_1H	−0.30	−0.50	0.20	0.06
	ϵ_3H	0.32	−0.25	0.57	0.06
	ζ_2H	0.37	−0.05	0.42	0.14
	ζ_3H	−0.09	0.11	0.20	0.08
Thr-68	βH	−0.05	−0.15	0.10	0.02
	γH_3[e]	0.00	−0.12	0.12	0.01
Thr-74	NH	0.17	−0.05	0.22	0.04
Tyr-75	δ_1H	0.20	1.51	−1.31	0.26
	δ_2H	−0.41	0.87	−1.28	0.69
	ϵ_1H	−0.56	2.44	−3.00	0.47
Lys-93	NH	0.43	0.20	0.23	0.03
Met-96	NH	0.27	1.44	−1.17	0.62
Lys-99	NH	0.85	0.37	0.48	0.13
	β_2H	0.70	0.46	0.24	0.09
Leu-100	$\delta_2 H_3$[e]	−0.33	−0.69	0.36	0.11
Ala-101	NH	−0.03	−0.18	0.15	0.05
	βH_3[e]	0.04	−0.07	0.11	0.02
Gly-103	α_2H	−0.21	−0.31	0.10	0.03
Leu-111	β_2H	−0.45	−0.01	−0.44	<0.01
	$\delta_1 H_3$[e]	−0.74	−1.40	0.67	0.26

[a] Protons listed are selected by the Equation 8.
[b] Observed chemical shift differences in parts per million measured at pH 6, 30 °C and pH 5.5, 30 °C for reduced and oxidized protein, respectively.
[c] Calculated dipolar shifts, $\Delta pc,x$, obtained by using the optimized **g**-tensor (50 NH in Table 1) and X-ray coordinates (Benning et al., 1991).
[d] The maximum pseudocontact shifts at the proton position calculated from Equation 7 and optimized **g**-tensor parameter (Table 1) with δl = 0.3 Å.
[e] The calculated shifts for benzoic fast-flipping protons and methyl protons were averaged.

imidazole ring of His-17 and result in the rearrangement of the hydrogen bond network with a change in the oxidation state.

The region on the left side of the heme (Fig. 5) involves eight residues, Thr-74, Tyr-75, Lys-93, Met-96, Phe-98, Lys-99, Leu-100, and Ala-101, which are associated with the Fe-S of Met-96 ligand. The aromatic OH of Tyr-75 and O_γH of Thr-94 are within hydrogen bond distance to an internal water molecule, which, in turn, is close to the CO of propionate 6. The NH of Gly-95 is hydrogen bonded directly to the propionate 6 carboxyl oxygen. There is a hydrogen bond between the NH of Leu-100 and the carbonyl of Val-76. These small local structural changes are suggested to be due to the Fe-S bond of Met-96 and the hydrogen bond rearrangements with the change in oxidation state.

The third region around the crevice structure of the protein includes residues in the 40s, 50s, and 60s (Fig. 5), and is equivalent to that observed by Feng et al. (1990). From the X-ray structure (Benning et al., 1991), in the sensitive segment from Tyr-53 to Trp-67, both Tyr-53 and Trp-67 are hydrogen bonded to the heme propionate 7 carboxyl; the NH of Ile-57 and the NH of Lys-54 are within hydrogen bond distance to both internal water molecules, which are close to the heme propionate 6 carboxyl oxygens. The segment from Gly-42 to Tyr-48 underlies propionate 7 and the aromatic group of Trp-67, and there are hydrogen bonds from the side-chain protons of Arg-43 to the propionate 7 carboxyl. The structural changes with oxidation in this region are suggested to be due to some changes in the heme propionate group and/or changes in position or number of the internal water molecules, which results in the rearrangement of the hydrogen bond network.

Recently, Qi et al. (1994) reported that the number and positions of structural waters vicinal to the heme group in horse cytochrome

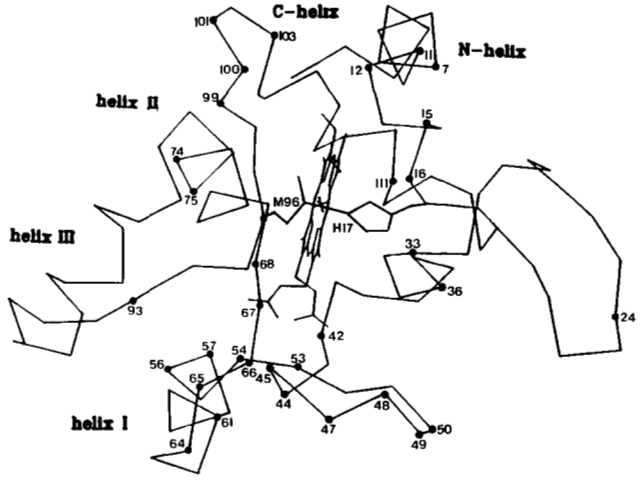

Fig. 5. α-Carbon model of *R. capsulatus* ferrocytochrome c_2 from the X-ray crystal coordinates (Benning et al., 1991). The position of the heme prosthetic group and the N-terminal, C-terminal, and I, II, III helices are shown. Positions of residues (●) selected by Equation 8 are indicated in this figure.

c in solution changed with oxidation state. Four internal water molecules were found to be close to the heme group in *R. capsulatus* ferrocytochrome c_2 by X-ray crystallography (Benning et al., 1991). These observations indicate that buried water molecules close to the heme group should play important roles in the redox process. In this study, several redox-sensitive protons listed in Table 2 are related to the four internal water molecules in *R. capsulatus* cytochrome c_2, as shown in Table 3.

For *R. capsulatus* cytochrome c_2, there is excellent agreement between the calculated and observed paramagnetic shifts over large portions of the protein, in spite of the use of X-ray crystal coordinates of the reduced form of protein. Furthermore, for the residues of the main heme ligands, such as His-17 and Ser-18, there is good agreement between calculated and experimental chemical shifts for amide, α, and β protons (Fig. 3). At the level of detection in this type of NMR experiment, it can be suggested that the average position of the heme center (Fe) has no significant movement. If there is a change in the position of the heme center (Fe) with respect to the porphyrin ring and axial ligands, then a chemical shift effect would be expected to accompany the change of oxidation state for a large number of residues (Kurland & McGarvey, 1970; Shulman et al., 1971; Horrocks & Greenberg, 1973; Wüthrich & Baumann, 1974; LaMar & Walker, 1979). For the heme aromatic ring and heme propionates, there may be some changes with the change of oxidation state, as discussed previously.

Table 3. *Bound internal waters and redox-sensitive protons in Rhodobacter capsulatus cytochrome* c_2[a]

Water	Bond to heme	Hydrogen bond	Sensitive proton
1 (31H)	Propionate 6:O_1	Tyr-75:O_η	Tyr-75:δ_1H
			:δ_2H
			:ϵ_1H
		Thr-94:O_γ	
2 (43H)	Propionate 6:O_1	Ile-57:N	Ile-57:NH
		Lys-93:CO	Lys-93:NH
3 (45H)	Propionate 6:O_2	Lys-54:N	Lys-54:NH
4 (18H)	Propionate 7:O_2	Arg-43:N_ϵ	
		Tyr-53:O_η	Tyr-53:δ_1H
			:δ_2H
			:ϵ_2H

[a] Four bound internal waters to be within hydrogen bonding distance in reduced *R. capsulatus* cytochrome c_2 (Benning et al., 1991) are listed, along with redox-sensitive protons from Table 2, which may relate to these hydrogen bonds. The water molecular names shown in parentheses are from the Brookhaven Protein Data Bank.

The N-terminal helix 3–13 and C-terminal helix 103–115 do not have significant differences between calculated and observed dipolar chemical shifts except for Asn-11, Lys-12, Gly-103, and Leu-111. Some long-range NOEs between both helices were obtained in the NMR experiments for reduced and oxidized forms (Gooley et al., 1991; D. Zhao, P.R. Gooley, M.A. Cusanovich, N.E. MacKenzie, unpubl.), indicating that both helices form a protective screen for the back side of the heme. This observation is similar to that found from the measurement of NH exchange rates, which showed that the folding equilibrium for N- and C-terminal helices are similar for both oxidized and reduced forms (Gooley et al., 1991). However, residues Asn-11 and Lys-12 in the N-terminal helix do have large differences (Table 2), which can be explained readily as a result of the close proximity of the residues to the bond between Cys-13 and the heme. The differences for Gly-103 and Leu-111 in the C-terminal helix are not considered significant (Table 2). Thus, it can be suggested that local structures of N- and C-terminal helices are overall the same for the oxidized and reduced cytochrome c_2.

It is now possible to discuss the relationship between the **g**-tensor values and the reported NH exchange values (Gooley et al., 1991). The determination of individual hydrogen-deuterium exchange rate constants of the NH protons can provide information about the stability of hydrogen bonds in the protein. As discussed previously (Gooley et al., 1991), the free energy difference, ΔG_{op}, between the open and closed forms of a protein can be determined from K_{op} the local unfolding equilibrium constant:

$$\Delta G_{op} = -RT \ln(K_{op}).$$

With a change in the oxidation state of the protein, the changes to the local unfolding equilibrium constant can be used to determine the difference in ΔG_{op}:

$$\delta\Delta G_{op} = -RT\,\delta(\ln K_{op}) = -RT \ln(k_m^1/k_m^2),$$

where k_m^1 and k_m^2 are the exchange rate constants for the same NH proton in the reduced and oxidized forms of the protein. If the open forms of these two states differ structurally, exchange may occur by different apparent rate constants, which could be reflected in $\delta\Delta G_{op}$. However, it has been suggested that the interpretation of these values should be approached cautiously and that the significance may only point to structurally important regions of the protein (Englander et al., 1983; Wand et al., 1986).

A list of redox-dependent backbone protons selected by Equation 8 were compared with the results from NH exchange determination (Gooley et al., 1991) shown in Table 4. The NH exchange values, $\delta\Delta G_{op}$, are based on the hypothesis that there is no structural change at this hydrogen bond position, whereas the **g**-tensor results point out which residue has some significant (by our cri-

Table 4. *Comparison of backbone protons selected by Equation 8 with the results from NH exchange*

Redox-dependent proton[a]				NH exchange[b]	
Proton		Δ (ppm)[c]	%[d]	Residue	$\delta\Delta G_{op}$[e]
Asn-11	NH	0.12	200		
	αH	0.08	160		
Lys-12	αH	0.07	63	Lys-14	1.7
Thr-15	αH	0.11	110	His-17	3.3
Cys-16	αH	0.71	186	Ser-18	1.8
				Gly-34	2.0
Asn-36	NH	0.27	150	Leu-37	3.5
Gly-42	NH	0.03	100		
	αH	0.02	100	Arg-43	2.6
Thr-44	αH	0.04	200	Ala-45	3.6
				Gly-46	3.1
				Thr-47	1.5
Lys-54	NH	.16	133		
Ser-56	NH	0.15	500		
Ile-57	NH	0.19	316	Ile-57	2.4
				Val-58	2.8
				Leu-60	2.5
Gly-61	αH	0.06	300	Gly-61	2.6
Gly-64	αH	0.04	200		
Phe-65	NH	0.02	100		
	αH	0.02	100		
Ala-66	NH	0.05	250		
	αH	0.03	100		
Trp-67	NH	0.03	75		
Thr-74	NH	0.13	260	Val-76	1.8
				Lys-77	2.1
				Phe-82–Leu-87	>1.6
Lys-93	NH	0.15	375		
Met-96	NH	0.50	79		
Lys-99	NH	0.30	214	Leu-100	2.6

[a] Backbone protons selected by Equation 8.
[b] Obtained from Gooley et al. (1991). There is no significant result from NH exchange for residues 62–73.
[c] $\Delta = |\Delta obs - \Delta pc,x| - |\delta\Delta pc + \delta| - 0.04$.
[d] $\% = \Delta/|\delta\Delta pc + \delta| * 100$.
[e] Unit is kcal·mol^{-1}.

teria) structural change with the change in oxidation state. We have found that the residues where there is structural change are not the same as those with a change in the NH exchange rate (Table 4), except for residues Ile-57 and Gly-61; however, it appears that the residues identified by the NH exchange are always closely related to those residues selected by the **g**-tensor method. It is evident that the structural change in a particular region affects the NH exchange in adjacent residues. For example, the structural changes in the region of Asn-11, Lys-12, Thr-15, and Cys-16 as identified by the **g**-tensor have the largest effect on NH exchange at Lys-14, His-17, and Ser-18.

We would suggest that the regions 11–18, 33–37, 42–47, 54–61, 74–77, and 93–101 are the structurally important regions contributing to the stability of *R. capsulatus* cytochrome c_2 and that there are small but significant (again by our criteria) changes with a change in the oxidation state. A comparison of the **g**-tensor and NH exchange results confirm, with only two exceptions, that there are no significant structural changes at the NH exchange positions, so the values of $\delta\Delta G_{op}$, which assumed no structural change, are reliable. Also, the small but significant structural change of residues in these regions would cause the change of the hydrogen-deuterium exchange rate constant of the NH proton, which indicates the change of stability of hydrogen bonds at these positions. In turn, the change of NH exchange rate within these regions should be reflected in the changes in **g**-tensor values because the two parameters found for these regions should be mutually interdependent.

In helices, the exchange of a hydrogen bonded N-H protons that stabilize the helix requires the breaking of the preceding hydrogen bond(s) and therefore segments of helices can act as cooperative unfolding units as shown in previous studies (Wagner & Wüthrich, 1982; Englander & Kallenbach, 1984; Wand et al., 1986). For example, the calculated dipolar shifts for the segment 82–87 of helix III are not significantly different from the observed paramagnetic shifts for the main-chain protons (Fig. 3), and are in complete agreement with the similar hydrogen-deuterium exchange rate values found for this helical segment in *R. capsulatus* cytochrome c_2 (Gooley et al., 1991).

Materials and methods

The optimized g-tensor

Williams et al. (1985) have pioneered the use of a calculated paramagnetic chemical shift of the side-chain protons on residues in the oxidized state to determine structural differences in solution for tuna ferro- and ferricytochrome *c*. Using the extensive main-chain chemical shift assignments for the two redox states of horse cytochrome *c*, Feng et al. (1990) used the same approach with the $C_\alpha H$ protons to calculate the **g**-tensor parameters for this protein. Because the positions of the main-chain protons are more precisely known in the protein, this analysis would give a more refined value of the **g**-tensor and hence more accurately calculated dipolar shifts values. The main-chain NH proton chemical shifts were not used as part of their reference set for the calculation of the **g**-tensor because it was suggested that the chemical shifts of the peptide NH protons are too sensitive to small structural changes.

Unlike these previous studies (Feng et al., 1990; Gao et al., 1991; Timkovich & Cai, 1993), we have opted to use the amide NH proton resonance chemical shifts to determine the optimized **g**-tensor parameters. The principal reasons are that, for main-chain proton conformation, the crystal structure is an accurate representation of the structure in solution (Gochin & Roder 1995), first because normally the coordinates of protons in crystal structure are used to calculate the pseudocontact shifts in solution; second, because of the inherent sensitivity of the NH proton to structural changes, this facilitates the choice of residues in which the NH group has undergone any structural change (or not); third, becuase the subset of residues chosen to calculate the **g**-tensor from the NH proton chemical shifts had to meet certain criteria—that of the chemical shift change synchronization of both proton and nitrogen within an identical amide group, described as follows.

The amide proton and nitrogen chemical shifts have been used to determine minimal structural changes in various peptides (Guiles et al., 1993). When there is some perturbation in the protein that results in an identical chemical shift change for both ^1H and ^{15}N in a particular residue, this suggests that there is not any significant local structural change in the region. In this study, we coin the use of the word "synchronization" to describe the case in which the NH proton and nitrogen have the same change in chemical shift as

a consequence of the change in oxidation state. From Equation 2, the values of the pseudocontact chemical shift ($\Delta pc,x$) should be the same for the amide proton and nitrogen in a given residue because the spin quantum numbers of ^1H and ^{15}N are the same and their position(s) with respect to the heme center is virtually identical. Thus, for synchronization

$$(\delta_{ox}^{1H} - \delta_{red}^{1H}) = (\delta_{ox}^{15N} - \delta_{red}^{15N}). \quad (3)$$

In order to determine the **g**-tensor parameters, the basic set of protons were chosen in residues far enough from the heme so that there is negligible Fermi contact contribution and, furthermore, no significant contribution to the chemical shift as a result of redox dependent structural (or conformational) changes. For *R. capsulatus* cytochrome c_2, a set of 50 backbone amide protons were chosen to determine the best fit **g**-tensor parameters: residues 2–10, 19–21, 23–26, 28–29, 38–41, 43, 46–48, 50–52, 61, 83–87, 89–92, 102, 105–110, 112–115. The amide protons selected are not close to the heme and are in well-defined structures that have the amide group chemical shift synchronization (see above). Therefore, the Fermi contact contribution Δc and the structural contribution Δs to the observed chemical shifts are both zero, as required for this procedure (Feng et al., 1990). The observed chemical shift difference would be given by:

$$\Delta obs = \delta_{ox} - \delta_{red} = \Delta pc,x. \quad (4)$$

In the selection of the 50 amide protons by chemical shift synchronization, it is possible that some of the proton/nitrogen pairs experience a change of chemical shift that was fortuitously equal, when indeed some structural/conformational change had occurred involving a particular residue. For these amide protons, the pseudocontact shifts determined by calculation and by experiment would not be equal because the latter would actually contain an unknown Δs component. To determine the sensitivity of the **g**-tensor parameters to this type of error, a subset of 43 were used in a separate calculation. In this case, seven protons (residues 19, 25, 41, 51, 85, 102, 108) were removed from the original 50, because they met the arbitrary error:

$$(\Delta pc,x)_{calc} - (\Delta pc,x)_{exp} > |0.050|. \quad (5)$$

Another subset containing 45 NH protons, eliminating residues 7, 21, 47, 52, and 115 from the original 50 NH protons, was also used. These residues are proximal to aromatic residues (as indicated from the X-ray determined structure) and therefore their chemical shift values may contain a contribution from ring current effects.

Least-squares fitting

The orientation and magnitude of the optimized **g**-tensor parameters for the oxidized cytochrome c_2 were determined from Equation 2, using the subsets of experimental paramagnetic chemical shift data for the selected NH protons (described above) of both oxidized and reduced *R. capsulatus* cytochrome c_2 in solution and the X-ray crystallographic coordinates of the reduced form of cytochrome c_2, which were obtained from the Brookhaven Protein Data Bank, and hydrogens were added in standard geometries by the software Insight II (Biosym Technologies). Here it was assumed that there is no change in structure between the oxidized and reduced states in solution and that the time-averaged structure in solution is the same as that of the reduced form in the solid state for these reference amide protons. This has been observed for other cytochromes *c*, such as horse cytochrome *c* (Feng et al., 1990). The calculation of dipolar shifts could be improved by using the refined coordinates of the solution structure rather than the crystal structure (Gochin & Roder, 1995). The best fit **g**-tensor parameters were found by minimizing the variance, χ^2, between the observed, $\Delta obs = \delta_{ox} - \delta_{red}$, and calculated dipolar chemical shifts, $\Delta pc,x$, for the reference sets of amide protons.

$$\chi^2 = \Sigma(\Delta obs - \Delta pc,x)^2. \quad (6)$$

To minimize the computerized iterative calculation, the **g**-tensor parameters (g_{ax}, g_{eq}, α, β, and γ) from the study of Mailer and Taylor (1972) were used as initial input values. These parameters were then optimized by minimizing χ^2, while systematically altering the five components of the **g**-tensor. Three rounds of optimization were performed. In the first round, each angle α and γ was incremented by 20 degrees from 0 degrees to 360 degrees, the angle β was incremented by 5 degrees from 0 degrees to 180 degrees and each anisotropy (g_{ax}, g_{eq}) by 0.05. In the second and third rounds, the increments were 2 degrees, 0.02 and 1 degree, 0.01, for the angles and anisotropies, respectively. During the search process, the χ^2 value reduced, by necessity, smoothly and converged to the given final global minimum value. In the Table 1, the results indicate that there is minimal difference in the **g**-tensor parameters determined from the original set of 50 residues and the subsequent subsets (45 NH, 43 NH, Table 1) in which residues were omitted for the reasons described above.

Structural changes

The optimized **g**-tensor was then used to calculate the dipolar shifts ($\Delta pc,x$) for all the protons in the *R. capsulatus* cytochrome c_2. A comparison between the calculated dipolar values and the observed values for individual protons identifies the protons that experience significant chemical shifts due to structural changes. However, because the $|\Delta obs - \Delta pc,x|$ value for a particular proton, as an indication of the amount of structural change, is related to the proton positional coordinates with the heme center of the protein, it is necessary to define a criterion to evaluate the significance of the difference with respect to a structural change. Our procedure was similar to that used by Feng et al. (1990):

$$|\delta\Delta pc| = \{|\partial\Delta pc/\partial r| + |\partial\Delta pc/r\partial\theta| + |\partial\Delta pc/r\sin\theta\partial\phi|\}\delta l. \quad (7)$$

The uncertainty in the calculated dipolar chemical shift, $\delta\Delta pc$, is determined with respect to the positional uncertainties of r, θ, ϕ, and the uncertainty in the crystallographic coordinates, δl. The space gradient of Δpc is different for each proton within the protein structure due to the individual position with respect to the unpaired electron of Fe(III) in the heme. The uncertainty in Δpc, as defined in Equation 7, was calculated for all protons using δl = 0.3 Å, which corresponds to a 0.5 Å displacement in any direction in real space. The observed and calculated shift differences as well as the values of $\delta\Delta pc$ are given in Table 2 for those protons with significant differences between the calculated and observed chemical shifts.

The selection of protons where the difference in chemical shift represents a significant structural change was somewhat different from that of Feng et al. (1990) or Gao et al. (1991).

$$\frac{(|\Delta obs - \Delta pc,x| - |\delta\Delta pc + \delta| - 0.04)}{|\delta\Delta pc + \delta|} \times 100\% > 50\%. \quad (8)$$

In Equation 8, the difference between ($\Delta obs - \Delta pc,x$) and $\delta\Delta pc$, the uncertainty in the calculated dipolar shift at the 0.3-Å displacement, and δ, the estimated non-pseudocontact shift, represents the significance of the difference between the observed and calculated chemical shifts with the uncertainty in the calculated dipolar shift. In this case, we set the δ as 0.01 ppm. For the value $|\Delta obs - \Delta pc,x| - |\delta\Delta pc + \delta|$ to be significant, it, in turn, must be larger than the experimental error 0.04 ppm (0.02 for each of Δobs and $\Delta pc,x$). This value is compared as a ratio to ($\delta\Delta pc + \delta$) and we have defined a significant structural change where the ratio, expressed as a percentage, is greater than 50%. In Equation 8, the larger the uncertainty in $\delta\Delta pc$, the smaller the percentage determined from Equation 8 and the more *unlikely* the difference, $\Delta obs - \Delta pc,x$, would be due to a structural change. Also the smaller the difference, $|\Delta obs - \Delta pc,x| - |\delta\Delta pc + \delta|$, with respect to 0.04, the smaller the percentage given by Equation 8 and again the *less likely* the difference would reflect a structural change. This type of selection, or filter, gave results for our data that were virtually identical to those in which the five **g**-tensor components (Feng et al., 1990) were used.

Acknowledgments

This work was supported in part by a grant from the NIH GM21277 to M.A.C. We thank Drs. Terrance E. Meyer, Michael S. Caffrey, and Frances Ann Walker for helpful and meaningful discussions.

References

Benning MM, Wesenberg G, Caffrey MS, Bartsch RG, Meyer TE, Cusanovich MA, Rayment I, Holden HM. 1991. Molecular structure of cytochrome c_2 isolated from *Rhodobacter capsulatus* determined at 2.5 Å resolution. *J Mol Biol 220*:673–685.

Bhatia GE. 1981. Refinement of the crystal structure of oxidized *Rhodospirillum rubrum* cytochrome c_2 [thesis]. San Diego, California: University of California, San Diego.

Caffrey MS, Davidson E, Cusanovich MA, Daldal F. 1992. Cytochrome c_2 mutants of *Rhodobacter capsulatus*. *Arch Biochem Biophys 292*:419–426.

Cusanovich MA, Meyer TE, Tollin G. 1988. *c*-Type cytochromes: Oxidation–reduction proteins. In: Eichhorn GL, Manzilli LG, eds. *Advances in inorganic biochemistry, heme proteins 7*. New York: Elsevier. pp 37–92.

Cutler RL, Pielak GJ, Mauk AG, Smith M. 1987. Replacement of cysteine-107 of *Saccharomyces cerevisiae* iso-1-cytochrome *c* with threonine: Improved stability of the mutant protein. *Protein Eng 1*:95–99.

Englander SW, Kallenbach NR. 1984. Hydrogen exchange and structural dynamics of proteins and nucleic acids. *Q Rev Biophys 16*:521–655.

Englander JJ, Rogero JR, Englander SW. 1983. Identification of an allosterically sensitive unfolding unit in the nemoglobin. *J Mol Biol 169*:325–344.

Feng Y, Roder H, Englander SW. 1990. Rodox-dependent structure change and hyperfine nuclear magnetic resonance shifts in cytochrome *c*. *Biochemistry 29*:3494–3504.

Feng Y, Roder H, Englander SW, Wand AJ, Di Stefano DL. 1989. Proton resonance assignments of horse ferricytochrome *c*. *Biochemistry 28*:195–203.

Gao Y, Boyd J, Pielak GJ, Williams RJP. 1991. Comparison of reduced and oxidized yeast iso-1-cytochrome *c* using proton paramagnetic shifts. *Biochemistry 30*:1928–1934.

Gochin M, Roder H. 1995. Protein structure refinement based on paramagnetic NMR shifts: Applications to wild-type and mutant forms of cytochrome *c*. *Protein Sci 4*:296–305.

Gooley PR, Caffrey MS, Cusanovich MA, MacKenzie NE. 1990. assignment of the ^{1}H and ^{15}N NMR spectra of *Rhodobacter capsulatus* ferrocytochrome c_2. *Biochemistry 29*:2278–2290.

Gooley PR, Zhao D, MacKenzie NE. 1991. Comparison of amide proton exchange in reduced and oxidized *Rhodobacter capsulatus* cytochrome c_2. *J Biomol NMR 1*:145–154.

Guiles RD, Basus VJ, Sarma S, Malpure S, Fox KM, Kuntz ID, Waskell L. 1993. Novel heteronuclear methods of assignment transfer from a diamagnetic to a paramagnetic protein: Application to rat cytochrome b_5. *Biochemistry 32*:8329–8340.

Horrocks WD Jr, Greenberg ES. 1973. Evaluation of dipolar nuclear magnetic resonance shifts in low-spin hemin systems: Ferricytochrome *c* and metmyoglobin cyanide. *Biochim Biophys Acta 322*:38–44.

Kurland RJ, McGarvey BR. 1970. Isotropic NMR shifts in transition metal complexes: The calculation of the Fermi contact and pseudocontact terms. *J Magn Reson 2*:286–301.

LaMar GN, Walker FA. 1979. Nuclear magnetic resonance of paramagnetic metalloporphyrins. In: Dolphin D, ed. *The porphyrins, vol 4*. New York: Academic Press. pp 61–157.

Mailer C, Taylor CPS. 1972. Electron paramagnetic resonance study of single crystals of horse heart ferricytochrome *c* at 4.2°K. *Can J Biochem 50*:1048–1055.

Qi PX, Urbauer JL, Fuentes EJ, Leopold MF, Wand AJ. 1994. Structural water in oxidized and reduced horse heart cytochrome *c*. *Structure Biology 1*:378–381.

Salemme FR, Kraut J, Kamen MD. 1973. Structural bases for function in cytochrome *c*. *J Biol Chem 248*:7701–7716.

Shulman RG, Glarum SH, Karplus M. 1971. Electronic structure of cyanide complexes of hemes and heme protein. *J Mol Biol 57*:93–115.

Takano T, Dickerson RE. 1981a. Conformation change of cytochrome *c*. *J Mol Biol 153*:79–94.

Takano T, Dickerson RE. 1981b. Conformation change of cytochrome *c*. *J Mol Biol 153*:95–115.

Timkovich R, Cai M. 1993. Investigation of the strucure of oxidized *Pseudomonas aeruginosa* cytochrome *c*-551 by NMR: Comparison of observed paramagnetic shifts and calculated pseudocontact shifts. *Biochemistry 32*:11516–11523.

Wagner G, Wüthrich K. 1982. Amide proton exchange and surface conformation of the basic pancreatic trypsin inhibitor in solution. *J Mol Biol 160*:343–361.

Wand AJ, Di Stefano DL, Feng Y, Roder H, Englander SW. 1989. Proton resonance assignments of horse ferrocytochrome *c*. *Biochemistry 28*:186–194.

Wand AJ, Roder H, Englander SW. 1986. Two-dimensional ^{1}H NMR studies of cytochrome *c*: Hydrogen exchange in the N-terminal helix. *Biochemistry 25*:1107–1114.

Williams G, Clayden NJ, Moore GR, Williams RJP. 1985. Comparison of the solution and crystal structures of mitochondrial cytochrome *c*. *J Mol Biol 183*:447–460.

Wüthrich K, Baumann R. 1974. Hyperfine shifts of the ^{13}C-NMR. in protoporphyrin IX iron (III) dicyanide and deuteroporphyrin IX iron (III) dicyanide. *Helv Chem Acta 57*:336–350.